JOURNAL OF CATALYSIS **167,** 354–363 (1997)
ARTICLE NO. CA971577

The Characterization of $BaCO_3$-Modified LaOF Catalysts for the OCM Reaction

C. T. Au,[1] Y. Q. Zhang, H. He, S. Y. Lai, and C. F. Ng

Chemistry Department and Centre for Surface Analysis and Research, Hong Kong Baptist University, Kowloon Tong, Hong Kong

Received May 9, 1996; revised November 6, 1996; accepted December 20, 1996

In this paper, $BaCO_3$ is reported to be a good promoter for rhombohedral LaOF. With the addition of 5–20 mol% $BaCO_3$, methane conversion at 800°C was increased by ca. 40% with only slight loss in C_2 selectivity. At $CH_4:O_2:N_2 = 2.6:1:12$ and a contact time of 0.6 g s ml^{-1}, the methane conversion was 36.1%, while the C_2 selectivity was 45.3%, giving a C_2 yield of 16.4% over the 10 mol% $BaCO_3$/LaOF catalyst at 800°C. Comparing to LaOF, there was a 30% increase in C_2 yield. Moreover, similar to the case of $BaCO_3$/LaOBr, the C_2H_4/C_2H_6 ratio was enhanced by the presence of 5–20 mol% $BaCO_3$. The loaded barium was found to remain on the surface of the catalyst. XRD, O_2-TPD, and CO_2-TPD studies revealed that the $BaCO_3$/LaOF catalysts changed greatly in composition, surface site basicity, and active site concentration during OCM reaction. *In situ* **Raman studies disclosed that at 700°C under CH_4/O_2 (2.6/1), O_2^{2-} species were present on the 10 mol% $BaCO_3$/LaOF catalyst, while none was observed on LaOF. We conclude that the enhancement in methane conversion over the 5–20 mol% $BaCO_3$/LaOF catalysts was due to the generation of surface $BaCO_3$ clusters on LaOF, which could decompose at the temperature range (700–850°C) adopted for OCM reaction to give BaO entities capable of activating O_2 to adsorbed O_2^{2-}.**

INTRODUCTION

In the past 15 years, considerable progress has been made in the search for active and selective catalysts for the oxidative coupling of methane (OCM). Chlorine had been introduced as promoter into catalysts or reaction stream by many investigators (1–11). Conway and Lunsford (11) paid particular attention to Li/Mg catalysts promoted with Cl^- and observed good activity and selectivity but poor active lifetime because of the loss of lithium and chloride at high temperature. In comparison, the use of other halogen ions such as F^- and Br^- in the modification of OCM catalysts has not been widely studied. Otsuka *et al.* (10) carried out OCM reaction with NiO catalysts promoted by LiF, LiCl, and LiBr. The NiO–LiF catalyst gave a CH_4 conversion of 20% and a C_2 selectivity of 26%. Loading alkaline earth halides (F^-, Cl^-, and Br^-) on CaO and MgO, Fujimoto *et al.* (12) observed that the ability of the oxides in decomposing methane diminished, resulting in the suppression of methane deep oxidation. Recently, Zhou *et al.* (13, 14) developed a series of fluoro-oxide catalysts which worked at lower temperature and showed good activity, selectivity, and stability for OCM reaction.

Earlier, we reported the performance of LaF_3/La_2O_3 catalysts in which rhombohedral LaOF was proposed to be the active phase (15). It was suggested that O_s^- species formed over LaOF are the active sites for OCM. It is expected that due to the deficiency of F^-, the LaOF lattice contains vacancies which can trap holes and electrons, resulting in the generation of active oxygen species responsible for the activation of methane. In another study, we observed a striking enhancement of ethene formation for the OCM reaction when LaOBr was promoted with $BaCO_3$ (16). A solid-state reaction occurred between $BaCO_3$ and LaOBr. It was suggested that defect sites formation accompanying this reaction interacted with O_2 to form O_2^{2-} species that were responsible for the high C_2H_4/C_2H_6 ratio in the OCM product. A systematic study of the effect of $BaCO_3$ modification of the surface of lanthanum oxyhalides has been undertaken. In this paper, the effect of $BaCO_3$ interaction with LaOF is reported.

EXPERIMENTAL

The catalysts were synthesized using a method similar to that employed in synthesizing $BaCO_3$/LaOBr catalysts (16). The chemicals (purity >99.9%) used in the preparation of the catalysts were products of Johnson Matthey & Co. Ltd. Rhombohedral LaOF was prepared by heating a ground mixture of La_2O_3 and LaF_3 in 1 : 1 molar ratio in air in a furnace at 800°C for 6 h. The $BaCO_3$/LaOF catalysts were prepared by mixing LaOF powder with the correct proportion of $BaCO_3$ in the form of aqueous suspension. After water evaporation, the mixture was ground and dried overnight in an oven at 110°C and pressed into small pellets before being calcined at 800°C for 6 h. The pellets were crushed and sieved to a grain size of 40–60 mesh.

[1] To whom correspondence should be addressed at Department of Chemistry, Hong Kong Baptist University, Kowloon Tong, Hong Kong. Fax: (852)23397348.

0021-9517/97 $25.00

The O_2 (99.7%), CH_4 (99.9%), C_2H_6 (99.0%), and N_2 (99.99%) gases were from Hong Kong Oxygen Ltd., while the $^{18}O_2$ (98%) isotope was purchased through the Hong Kong Special Gas Ltd. The gases were used without further purification.

Catalytic interactions were studied at 750 and 800°C using a laboratory scale fixed-bed reactor system operating under atmospheric pressure (15). The reactors were constructed of fused quartz. A thermocouple was placed in direct contact with the catalyst for accurate temperature measurement. The catalyst (0.5 g) was placed in the reactor and treated with a mixture of O_2 and N_2 (flow rate, 50 ml min^{-1}) at 750°C for 2 h before reaction. Products were analyzed, usually 60 min after temperature stabilization, by on-line gas chromatography (Shimadzu GC-8APT). A Porapak Q column was used to separate CH_4, CO_2, C_2H_4, and C_2H_6. A 5 A molecular sieve column was used (in parallel) to separate N_2, O_2, CH_4, and CO.

The phase composition of the catalysts was determined by X-ray diffraction (D-MAX, Rigaku), whereas X-ray photoelectron spectroscopy (Leybold Heraeus-Shenyang SKL-12) was used to characterize the catalyst surface. *In situ* Raman experiments were performed in Xiamen University (P. R. China) using the Raman spectrometer SPEX Ramalog-6.

The $^{18}O/^{16}O$ isotope exchange experiments were performed at atmospheric pressure at 750 and 800°C, using a pulse reaction system (similar to the one described previously (17)) with pulse size of 1.12 μmol. The catalyst (0.2 g) was placed in a quartz reactor and treated first with pure O_2 (1 h) and then N_2 (1/2 h) (flow rate, 50 ml min^{-1}) at 750°C before isotope exchange experiments. The effluent from the reactor was directed to a GC–MS system (HP G1800A GCD) for analysis.

Temperature-programmed desorption (TPD) of CO_2 was used to gauge the surface basicity of the catalysts. The desorption of O_2 was used also to characterize the surface of the catalysts. The catalyst (about 0.2 g) was packed and secured by quartz wool in a quartz reactor (i.d., 4 mm). It was pretreated by a flow of dry He (30 ml min^{-1}) at 800°C for 1 h to remove adsorbates. The catalyst was then exposed to CO_2 (or O_2) at 800°C for 0.5 h and cooled to room temperature in CO_2 (or O_2). With the samples being heated at a rate of 13°C min^{-1} under a flow of helium, TPD spectra were recorded within a temperature range of 30 to 850°C. The desorbed gas was carried by the helium flow to a GC–MS system (HP G1800A GCD) for monitoring.

RESULTS

Catalytic Performance

Figure 1 shows the performance of the $BaCO_3$/LaOF catalysts at 800°C related to the amount of $BaCO_3$ added.

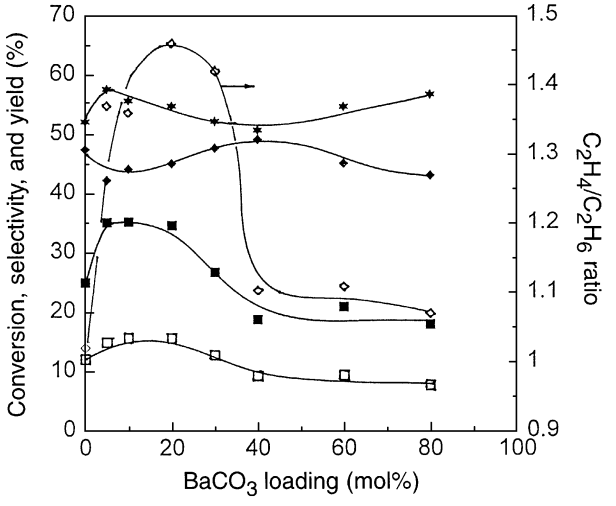

FIG. 1. The catalytic performance of $BaCO_3$/LaOF catalysts at 800°C related to $BaCO_3$ loading. ■, CH_4 conversion; ♦, C_2 selectivity; ★, CO_x selectivity; □, C_2 yield; ◊, C_2H_4/C_2H_6. (At 10 mol $BaCO_3$ loading, the specific activity of methane was 4.35×10^{17} molecules m^{-2} s^{-1}.)

For pure LaOF, methane conversion was ca. 25%; with the addition of $BaCO_3$, it reached a maximum value of ca. 35% over the range of $BaCO_3$ content of 5–20 mol%. Above 20 mol% $BaCO_3$, methane conversion decreased gradually to ca. 20% at 40 mol% $BaCO_3$ loading and remained roughly at this level up to 80 mol%. The C_2 selectivity changed little and stayed at around 45% within the 0–80 mol% loading range. At 20 mol% $BaCO_3$ loading, the C_2H_4/C_2H_6 ratio was ca. 1.45. For LaOF alone, it was ca. 1.0. Hence the addition of 5–20 mol% of $BaCO_3$ in LaOF could result in a gain of ca. 40% in both methane conversion and C_2H_4/C_2H_6 ratio but only slight loss (ca. 7%) in C_2 selectivity. The specific surface area of a LaOF catalyst after OCM reaction was ca. 10.8 m^2 g^{-1}. It decreased to ca. 6.4 and 3.0 m^2 g^{-1} when the $BaCO_3$ loading was 10 and 20 mol%, respectively. Hence the increase in methane conversion shown in Fig. 1 was not a consequence of an increase in specific surface area. Also, such a decrease (over 72% from 0 to 20 mol% $BaCO_3$ loading) in specific surface area had caused no drastic change in C_2 selectivity.

We chose the 10 mol% $BaCO_3$/LaOF for detailed investigation. Figure 2 shows that an increase in contact time (from ca. 0.2 to 1.4 g s ml^{-1}) resulted in a decrease in C_2 selectivity but an increase in C_2H_4/C_2H_6 ratio. This was because the increase in contact time promoted deep oxidation of C_2 hydrocarbon and dehydrogenation of C_2H_6. Figure 3 shows that the best reaction temperature for the catalyst was 800°C. At $CH_4 : O_2 : N_2 = 2.6 : 1 : 12$ and a contact time of 0.6 g s ml^{-1}, the methane conversion was 36.1%, while the C_2 selectivity was 45.3%, giving a C_2 yield of 16.4%. The corresponding rate of methane reaction was 2.69×10^{18} molecules g^{-1} s^{-1} or 4.35×10^{17} molecules m^{-2} s^{-1}.

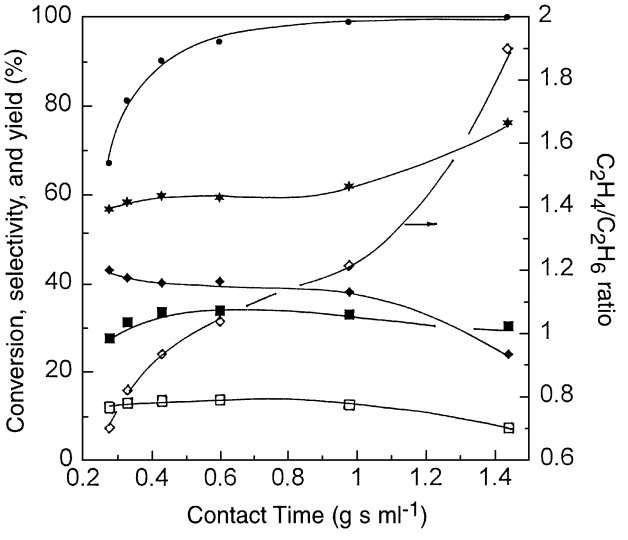

FIG. 2. The catalytic performance of a 10 mol% $BaCO_3$/LaOF catalyst at 800°C related to contact time. ■, CH_4 conversion; ●, O_2 conversion; ♦, C_2 selectivity; ★, CO_x selectivity; □, C_2 yield; ◊, C_2H_4/C_2H_6. (At a contact time of 0.6 g s m^{-2}, the specific activity of methane was 4.35×10^{17} molecules m^{-2} s^{-1}.)

XRD Studies

Figure 4a shows the phase composition of the $BaCO_3$/LaOF catalysts before the OCM reaction related to $BaCO_3$ loading. Between 5 and 40 mol% $BaCO_3$, the catalysts were composed of rhombohedral LaOF, hexagonal La_2O_3, hexagonal $La(OH)_3$, and cubic BaF_2. Only above 40 mol% $BaCO_3$ could the crystal phase of orthorhombic $BaCO_3$ be observed. Between 40 and 80 mol% $BaCO_3$, the catalysts were composed of LaOF, $BaCO_3$, La_2O_3, and $La(OH)_3$. At 80 mol%, no LaOF was detected and the composites were $BaCO_3$, BaF_2, La_2O_3, and $La(OH)_3$. The *d* values of the constituent compounds give no indication of any occurrence of lattice distortions.

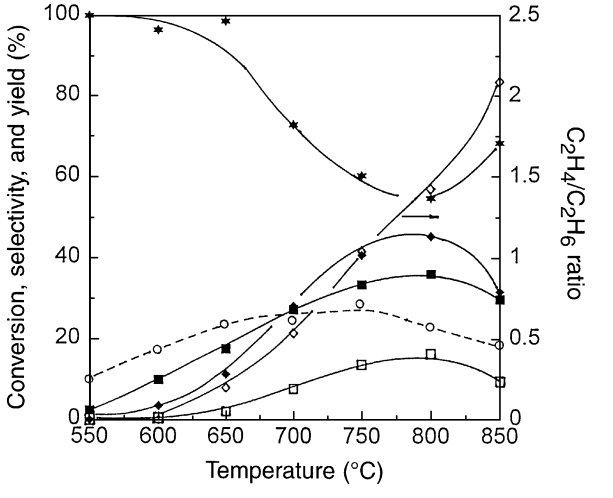

FIG. 3. The catalytic performance of a 10 mol% $BaCO_3$/LaOF catalyst related to reaction temperature. ■, CH_4 conversion; ♦, C_2 selectivity; ★, CO_x selectivity; □, C_2 yield; ◊, C_2H_4/C_2H_6. The CH_4 conversion (○) over a LaOF catalyst is also shown for comparison. (At 800°C, the specific activity of methane was 4.35×10^{17} molecules m^{-2} s^{-1}.)

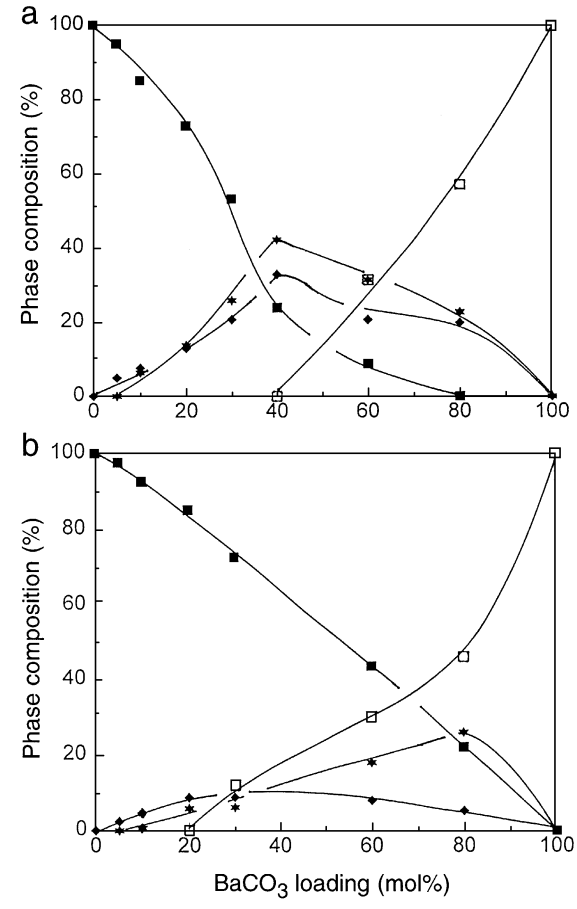

FIG. 4. Phase composition of $BaCO_3$/LaOF catalysts related to $BaCO_3$ loading (a) before and (b) after OCM reactions. ■, LaOF; ♦, $La_2O_3 + La(OH)_3$; ★, BaF_2; □, $BaCO_3$.

After the OCM reaction (Fig. 4b), LaOF remained as a component of the $BaCO_3$/LaOF catalysts. BaF_2 and $BaCO_3$ were observed above 20 mol% $BaCO_3$ loading. The amount of La_2O_3 and $La(OH)_3$ was greatly reduced when compared with that of Fig. 4a. At 10 mol% $BaCO_3$, no crystal phase of any barium compound was seen. Hence if barium compounds were present, they were well dispersed on the surface of LaOF. Again, the *d* values of the constituent compounds give no indication of lattice distortions.

XPS Studies

According to the XPS spectra, the La3$d_{5/2}$ peak was at ca. 834.0 eV binding energy with a satellite peak at ca. 837.6 eV. The F1*s* peak was at ca. 683.8 eV. The Ba3$d_{3/2}$ peak was at 779.5 eV for the 10 mol% $BaCO_3$/LaOF catalyst. The peaks changed little in position after OCM reaction. The O1*s* peaks showed two components which could be assigned

TABLE 1

Surface Elemental Composition of the Catalysts before (BR) and after (AR) the OCM Reaction, Based on the XPS Data

Catalysts	Ba (%)	F (%)	La (%)	O (%)	C (%)	F/La	Ba/La
LaOF (BR)	—	14.9	17.1	41.5	26.4	0.87	—
LaOF (AR)	—	8.5	10.7	40.5	40.3	0.79	—
10 mol% $BaCO_3$/LaOF (BR)	2.8	9.8	9.2	50.9	27.3	1.06	0.30
10 mol% $BaCO_3$/LaOF (AR)	2.4	6.5	5.9	40.6	44.5	1.10	0.41

to surface oxide O^{2-} and surface OH^- or CO_3^{2-}. The C1s peaks were at 284.4 and 289.1 eV, corresponding to surface CH_x and CO_3^{2-}, respectively (18). Table 1 shows the surface composition of the LaOF and 10 mol% $BaCO_3$/LaOF catalysts before and after the OCM reaction. Generally speaking, there was a large increase in surface carbon after the OCM reaction, confirming the accumulation of surface CH_x and carbonate generation during the OCM reaction. The small change in F/La ratio for the two catalysts before and after the OCM reaction suggests that there was little change in surface F composition during OCM reaction (over 8 h). For the 10 mol% $BaCO_3$/LaOF catalyst, the Ba/La ratio was, respectively, 0.3 and 0.4 before and after the OCM reaction.

$^{18}O/^{16}O$ Isotope Exchange Studies

The temperature dependence of the conversion of $^{18}O_2$ to isotope exchange products, viz. $^{18}O^{16}O$ and $^{16}O_2$, when pulsing $^{18}O_2$ over the LaOF and 10 mol% $BaCO_3$/LaOF catalysts, are summarized in Fig. 5. All possible oxygen molecules ($^{18}O_2$, $^{18}O^{16}O$, and $^{16}O_2$) were detected at the reactor outlet. The yield of $^{16}O_2$ over the two catalysts increased with increasing temperature and $^{16}O_2$ became the main product above 600°C (Fig. 5b). The yield of $^{18}O^{16}O$ passed through a maximum over both catalysts (Fig. 5c). With reference to the reaction scheme proposed by Winter (19, 20),

$$^{18}O_2 + {}^{16}O_{(s)} \rightleftharpoons {}^{18}O^{16}O + {}^{18}O_{(s)} \quad [1]$$

$$^{18}O^{16}O + {}^{16}O_{(s)} \rightleftharpoons {}^{16}O_2 + {}^{18}O_{(s)}, \quad [2]$$

one may assume that the exchange of oxygen proceeds stepwise and the formation of $^{16}O_2$ via the formation of $^{18}O^{16}O$ is a double exchange process. When the temperature increases, diffusion of surface $^{18}O_{(s)}$ species into the bulk becomes fast. The surface becomes depleted of $^{18}O_{(s)}$ species. Therefore, $^{16}O_2$ was the main product at temperatures higher than 500 and 600°C over LaOF and 10 mol% $BaCO_3$/LaOF, respectively, and the yield of $^{18}O^{16}O$ reaches a maximum. In other words, diffusion of oxygen species was facile inside the two catalysts above 700°C.

In Situ Raman Studies

In situ laser Raman spectroscopy has been applied to characterize surface dioxygen and carbonate species (Fig. 6). From Fig. 6a, one can see that no Raman band was observed over LaOF catalyst under a flow of oxygen (1 atm) at 700°C. At 500°C, a Raman band at 994 cm^{-1} was observed. At 300°C, bands were observed between 1000 to 1150 cm^{-1}. At 100°C, the bands within the 1000 to 1150 cm^{-1} range intensified. Exposure of the catalyst to a CH_4/O_2 (2.6/1) mixture at 700°C resulted in the existence

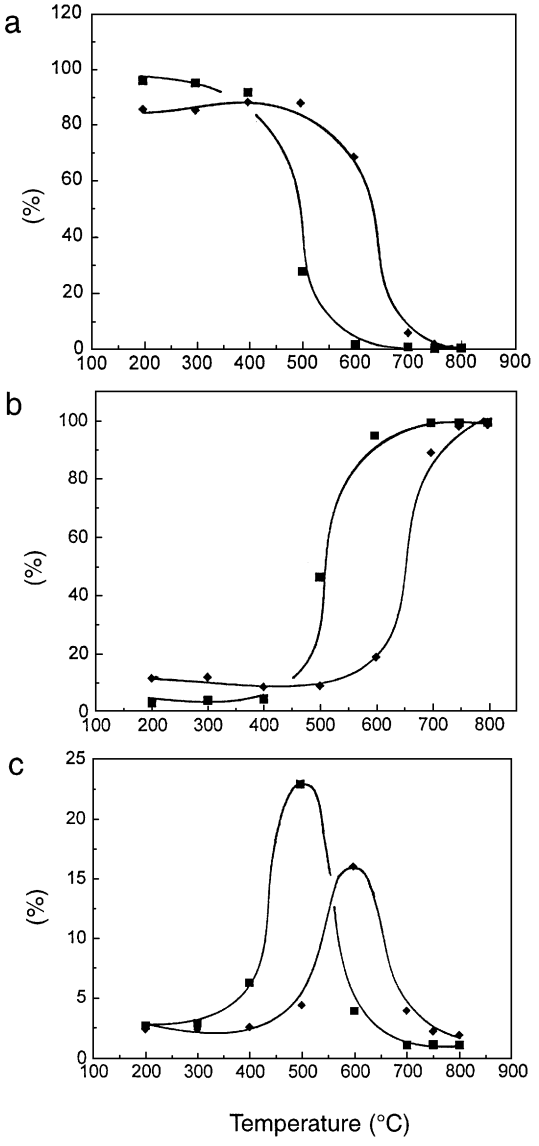

FIG. 5. The amount of (a) $^{18}O_2$, (b) $^{16}O_2$, and (c) $^{18}O^{16}O$ at the reactor outlet in $^{18}O/^{16}O$ isotope exchange experiments over (■) LaOF and (♦) 10 mol% $BaCO_3$/LaOF related to temperature.

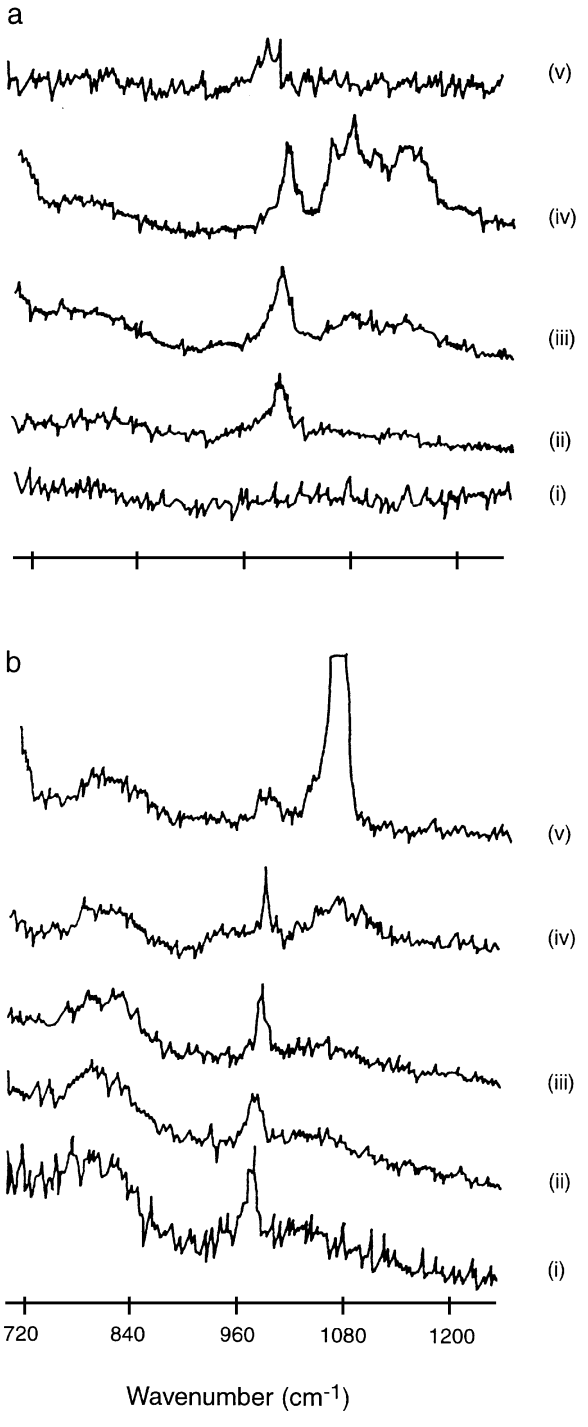

FIG. 6. Raman spectra obtained when (a) LaOF and (b) 10 mol% $BaCO_3$/LaOF catalysts were under (i) O_2 at 700°C, (ii) O_2 at 500°C, (iii) O_2 at 300°C, (iv) O_2 at 100°C, and (v) CH_4/O_2 (2.6/1) at 700°C.

of only one Raman band at 998 cm^{-1}. No bands due to the presence of CO_3^{2-} were detected.

For the 10 mol% $BaCO_3$/LaOF catalyst, weak Raman bands at ca. 800 and 976 cm^{-1} were observed under oxygen at 700°C. When the catalyst was cooled to 100°C, there

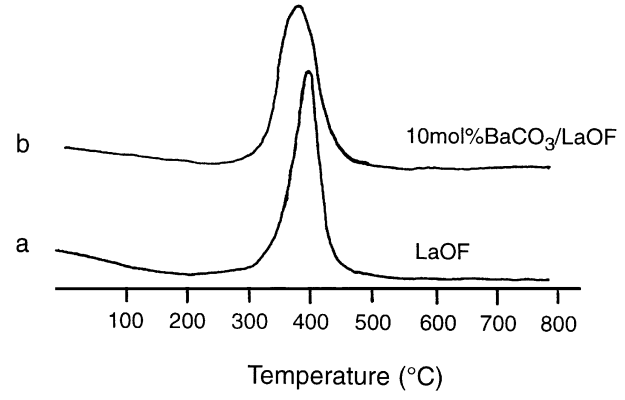

FIG. 7. O_2-TPD spectra over (a) LaOF and (b) 10 mol% $BaCO_3$/LaOF catalysts.

was enhancement in band intensity at 800 cm^{-1}, whereas between 1000 and 1100 cm^{-1}, a broad band appeared. Exposure of the catalyst to a mixture of CH_4/O_2 (2.6/1) at 700°C resulted in a strong band at 1058 cm^{-1}, signifying the generation of surface CO_3^{2-} species (21). Signals at 800 and 976 cm^{-1} were also observed (Fig. 6b).

O_2-TPD Studies

The O_2-TPD spectrum of LaOF before OCM reaction shows an oxygen desorption peak at 400°C. For a 10 mol% $BaCO_3$/LaOF catalyst, a wider oxygen desorption peak was observed at 374°C (Fig. 7). Compared with the fresh catalysts, the catalysts used in the OCM reaction could adsorb less amount of oxygen; the amount of O_2 desorbed in TPD studies was substantially less (Fig. 8). For the LaOF catalyst,

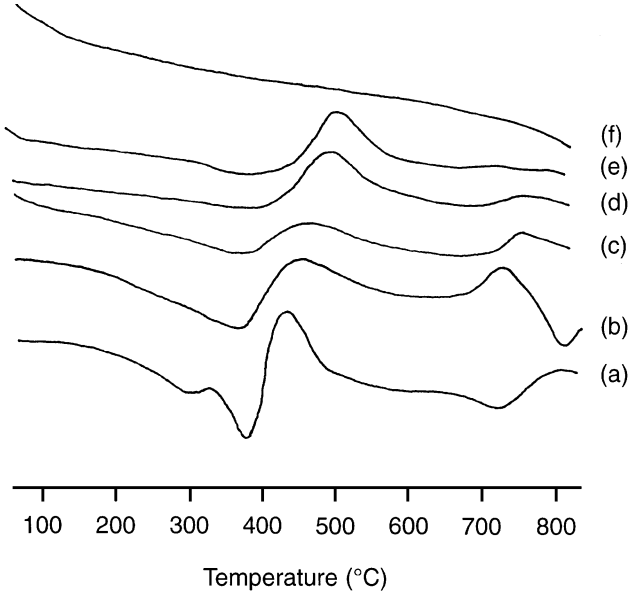

FIG. 8. O_2-TPD spectra over (a) LaOF, (b) 10 mol% $BaCO_3$/LaOF, (c) 20 mol% $BaCO_3$/LaOF, (d) 40 mol% $BaCO_3$/LaOF, (e) 60 mol% $BaCO_3$/LaOF, and (f) $BaCO_3$ catalysts used in the OCM reaction.

oxygen desorption started at 100°C and carried on in a gradual and continuous manner as the temperature rose. There was an oxygen desorption peak at ca. 424°C and desorption continued well above 800°C. For the $BaCO_3$/LaOF catalysts, oxygen desorption became significant above 350°C and continued as temperature rose to 800°C. Two distinct peaks were observed at 460 and 716°C for the 10 mol% $BaCO_3$/LaOF catalyst. The 460°C peak shift gradually to ca. 500°C as the amount of $BaCO_3$ in LaOF increased to 60 mol%. For the 716°C peak, it decreased in intensity and shifted to 765°C as the amount of $BaCO_3$ added rose to 40 mol%. For a 100% $BaCO_3$ sample, there was no oxygen desorption (Fig. 8).

CO_2-TPD Studies

CO_2-TPD studies revealed that there were sites with different strength of basicity on the surface of the LaOF and $BaCO_3$/LaOF catalysts (Fig. 9). For the LaOF catalyst, CO_2-TPD peaks were observed at ca. 400, 518, and 798°C. As the amount of $BaCO_3$ added increased, the 518°C peak increased in intensity. A pure $BaCO_3$ sample showed small CO_2 desorption at 570 and 755°C, but large CO_2 desorption above 850°C. Bulk $BaCO_3$ decomposes in air at about 990°C (22) and we ascribe the desorption above 850°C to bulk $BaCO_3$ decomposition. For the LaOF catalyst, there was no CO_2 desorption above 850°C. As $BaCO_3$ was added to LaOF, CO_2 desorption above 850°C was observed.

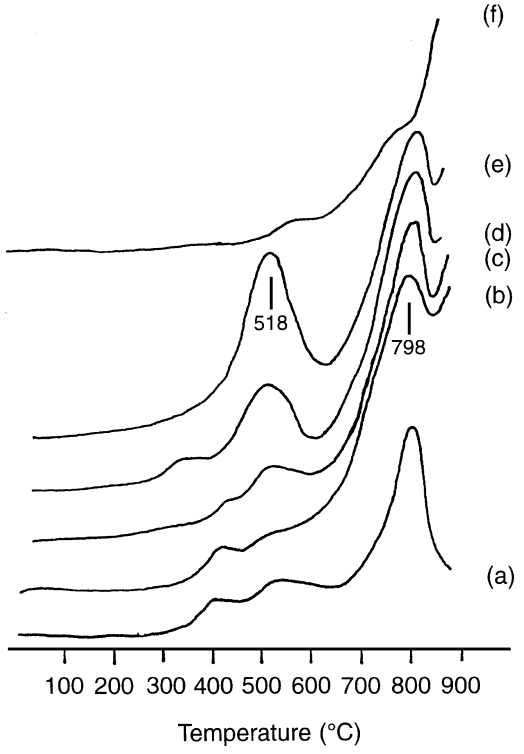

FIG. 9. CO_2-TPD spectra over (a) LaOF, (b) 10 mol% $BaCO_3$/LaOF, (c) 20 mol% $BaCO_3$/LaOF, (d) 40 mol% $BaCO_3$/LaOF, (e) 60 mol% $BaCO_3$/LaOF, and (f) $BaCO_3$ catalysts.

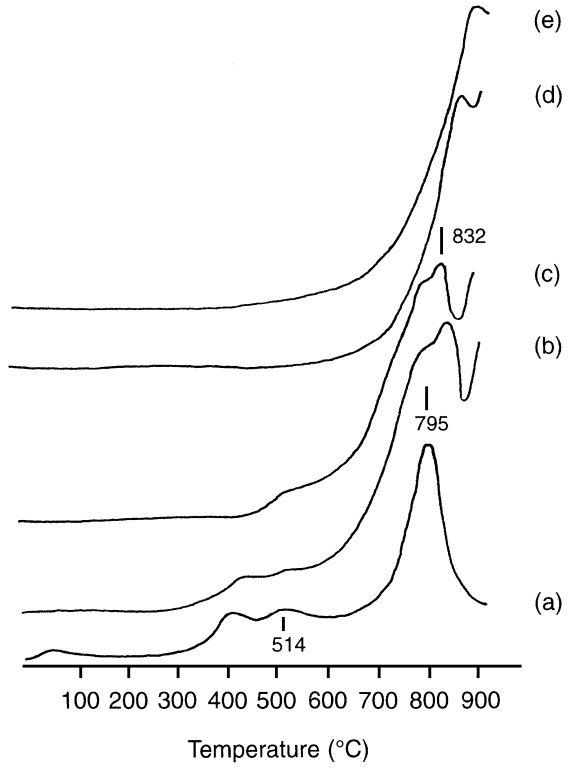

FIG. 10. CO_2-TPD spectra over (a) LaOF, (b) 10 mol% $BaCO_3$/LaOF, (c) 20 mol% $BaCO_3$/LaOF, (d) 40 mol% $BaCO_3$/LaOF, and (e) 60 mol% $BaCO_3$ catalysts used in the OCM reaction.

For the LaOF catalyst after OCM reaction (Fig. 10), CO_2 desorption peaks were observed at ca. 60, 405, 514, and 795°C, indicating the existence of four different types of basic site on the used LaOF. With the addition of $BaCO_3$, these CO_2-TPD peaks vanished gradually and there emerged another peak at temperature between 800 and 900°C. When the amount of $BaCO_3$ added was above 20 mol%, CO_2 desorption above 850°C became dominant. At 10 and 20 mol% $BaCO_3$, there were two types of CO_2-desorption between the 750 and 850°C temperature range: one at ca. 795°C and the other at 832°C. At 40 and 60 mol%, CO_2 desorption was above 850°C and out of the adopted temperature range for the OCM reaction.

DISCUSSION

Previously, we had shown that the catalytic performance of La_2O_3 for the OCM reaction could be promoted by LaF_3 and the rhombohedral LaOF generated in the LaF_3/La_2O_3 catalysts was suggested to be the active phase (15). When 5 to 20 mol% $BaCO_3$ was used to promote LaOF, there was an approximately 40% gain in methane conversion but relatively speaking, little decrease in C_2 selectivity (Fig. 1).

The net gain in C_2 yield was ca. 30%. We first envisaged that such gain in methane conversion was due to an increase in specific surface areas of the catalysts. We were intrigued to realize that there were in fact large decreases in specific surface areas when 10 and 20 mol% of $BaCO_3$ were added to LaOF. With such a drop in specific surface area, one would expect a large decrease in methane conversion based on the heterogeneous–homogeneous reaction scheme referred to by Lin *et al.* (23), Iwamatsu *et al.* (24) and us (15). In order to elucidate the specific nature of the $BaCO_3$/LaOF catalysts, we used a number of techniques to characterize the catalysts. XRD studies revealed that during catalyst preparation, there was interaction between the $BaCO_3$ and LaOF phases. Cubic BaF_2 phase was generated and part of LaOF was converted to La_2O_3 and $La(OH)_3$. Only above 40 mol% $BaCO_3$ loading could orthorhombic $BaCO_3$ crystal phase be observed (Fig. 4a). After the OCM reactions, crystal phases of BaF_2 and $BaCO_3$ were still detected above 20 mol% $BaCO_3$ loading (Fig. 4b). Hence, one can conclude that the large decrease in specific surface area of the $BaCO_3$/LaOF catalysts was due to sintering of barium compounds on the surface of the catalysts. For the 5 and 10 mol% $BaCO_3$/LaOF catalysts, we are sure that the barium compounds were well-dispersed on the surface as we did not detect any crystal phase of barium compounds after OCM reactions.

XPS studies of the LaOF and 10 mol% $BaCO_3$/LaOF catalysts showed that the surfaces of the two catalysts had undergone changes during the OCM reactions. The increase in Ba/La ratio over the $BaCO_3$/LaOF catalyst after the OCM reaction could be due to the La3$d_{5/2}$ signals being attenuated by the carbon species accumulated on the surface. This means that barium was on top of lanthanum. Ba^{2+} ions are bigger in size (25) (radius, 1.43Å) than La^{3+} ions (radius, 1.06Å) and carry smaller charge. If there was replacement of La^{3+} ions by Ba^{2+} ions in the lattices of lanthanum compounds, one would expect lattice enlargement of La_2O_3, $La(OH)_3$ and LaOF compounds. Since the *d* values (XRD studies) of the constituent compounds did not show any sign of lattice distortions, we conclude that the Ba^{2+} ions loaded on LaOF stayed largely on the surface of the $BaCO_3$/LaOF catalysts.

Based on the $^{18}O/^{16}O$ isotope exchange data, one can conclude that LaOF is more capable of activating O_2. Appearance of gaseous $^{16}O_2$ occurred at 400°C for LaOF and at 500°C for 10 mol% $BaCO_3$/LaOF. Hence below 600°C, gaseous oxygen could be activated 100°C lower on LaOF than on 10 mol% $BaCO_3$/LaOF. This is in good agreement with the observation that below 700°C, methane activation was higher over LaOF than over 10 mol% $BaCO_3$/LaOF as shown in Fig. 3. Above 650°C over the LaOF catalyst, O_2 conversion was nearly 100% and no increase in CH_4 conversion could be achieved above this temperature. Similarly, above 800°C over the 10 mol% $BaCO_3$/LaOF catalyst, CH_4 conversion stopped increasing due to the same reason. The drop in methane conversion above 750 and 800°C over LaOF and 10 mol% $BaCO_3$/LaOF, respectively was due to the increased consumption of oxygen in deep oxidation over the two catalysts at these high temperatures. The $^{16}O/^{18}O$ isotope exchange studies also suggest that below 700°C, the presence of barium compound(s) on LaOF hindered the activation of gaseous O_2. However, at or above 700°C and within the temperature range for effective OCM reaction, O_2 activation on the 10 mol% $BaCO_3$/LaOF catalyst was as effective when compared to the LaOF catalyst. Diffusion of oxygen species was facile inside the two catalysts. As discussed in our earlier paper, defects in the LaOF lattice could result in the generation of holes and electrons trapped in anion vacancies (15). The interaction of oxygen with hydrogen from methane might as well produce trapped electrons as suggested by Tench *et al.* (26). Interaction of O_2 with such defects could generate dioxygen species such as O_2^{2-}, O_2^{n-} $(1 < n < 2)$, O_2^- and $O_2^{\delta-}$ $(0 < \delta < 1)$. That trapped electrons can combine with O_2 to form partially reduced oxygen species has been suggested by Ito *et al.* (27) and Wang and Lunsford (28). We suggested that the migration of trapped electrons and O^{2-} ions to the surfaces of LaOF and $BaCO_3$/LaOF catalysts could produce sites suitable for O_2 activation. As one can see later, the *in situ* Raman results bear witness to such proposition.

Before discussing the *in situ* Raman results, we would like to show how the Raman bands were assigned. When electrons are added to O_2, the antibonding π^* is occupied and dioxygen species such as O_2^- and O_2^{2-} are produced, with the weakening of the O–O bond expected. Dioxygen species are known to absorb at 1550 cm^{-1} for O_2 (29–31), 1140 cm^{-1} for O_2^- (32, 33) and 850 cm^{-1} for O_2^{2-} (34, 35). For the Raman bands observed between 960 and 1100 cm^{-1} in Fig. 6, we assign them to O_2^{n-} $(1 < n < 2)$ species which are O_2^{2-} species perturbed in the direction of O_2^-. Similar suggestion had been made before by Lever *et al.* (36) and Valentine (37).

Hence the exposure of the LaOF catalyst to O_2 at 100°C could result in the generation of O_2^{n-} and O_2^- species (Fig. 6a). At 300°C under O_2, the intensities of the bands between 1020 and 1200 cm^{-1} reduced, indicating the decrease in concentration of O_2^{n-} and O_2^- species on the surface of the catalyst. At 500°C, only the band at 994 cm^{-1} due to O_2^{n-} remained. At 700°C, no Raman band was observed within the recorded range, viz. 720 to 1250 cm^{-1}. For a 10 mol% $BaCO_3$/LaOF catalyst, Raman bands at ca. 800, 976, and 1071 cm^{-1} were observed when the catalyst was under O_2 at 100°C (Fig. 6b). The 800 cm^{-1} band was due to O_2^{2-}, while the other two bands were due to O_2^{n-} species. The 1071 cm^{-1} band reduced in intensities at 700°C but the 800 and 976 cm^{-1} bands remained intact. O_2-TPD experiments of the two catalysts before the OCM reactions showed oxygen desorption peaks at 400 and 374°C, respectively, over

LaOF and 10 mol% $BaCO_3$/LaOF (Fig. 7). Based on the $^{18}O/^{16}O$ isotope exchange results (Fig. 5), we know that below 400°C, oxygen migration from the bulk to the surface of the two catalysts was insignificant. Hence the desorption of oxygen over the two catalysts was due to oxygen adsorbed on the surface. For the oxygen desorbed below 500°C, they are corresponding to the surface dioxygen species with Raman bands between 1000 and 1150 cm^{-1} (Fig. 6). They are surface O_2^{n-} and/or O_2^- species. No significant oxygen desorption could be observed from 500 to 800°C. However, for the LaOF catalyst, O_2^{n-} species with Raman band at 994 cm^{-1} was present at 500°C but not seen at 700°C. We speculate that at 700°C, O_2^{n-} species dissociated to monooxygen species O^- which are undetectable by Raman spectroscopy. Such conversion of dioxygen species to O^- centers had been reported before over a 20 mol% SrF_2/SmOF catalyst (38). It is interesting to note that under the OCM reaction condition at 700°C over LaOF, only a very weak band at 998 cm^{-1} but no band at 1058 cm^{-1} was detected (Fig. 6a (v)). One can conclude that no carbonate formation had occurred on the surface of LaOF during the OCM reaction. As for the 10 mol% $BaCO_3$/LaOF catalyst, a strong band at 1058 cm^{-1} due to CO_3^{2-} symmetric stretching vibration was observed under CH_4/O_2 (2.6/1) at 700°C. Since no such band was observed before CH_4/O_2 exposure, we conclude that the 10 mol% $BaCO_3$ loaded on LaOF had decomposed during catalyst preparation and the barium compound on the catalyst was in fact BaO. During the OCM reaction at 700°C, $BaCO_3$ was generated as a result of BaO interaction with the CO_2 produced in the OCM reaction. Hence the addition of 10 mol% $BaCO_3$ has two distinct effects on LaOF. First, it promoted O_2^{2-} generation, and second, it caused CO_3^{2-} formation during the OCM reaction at 700°C.

In good agreement with the $^{18}O/^{16}O$ studies, *in situ* laser Raman studies also showed that below 500°C, LaOF was more capable of activating O_2 (producing O_2^{n-} and O_2^-) than 10 mol% $BaCO_3$/LaOF (Figs. 6a and 6b). At or above 500°C, the $BaCO_3$-promoted LaOF catalyst was more capable of producing O_2^{2-} species. We propose that the presence of O_2^{2-} on 10 mol% $BaCO_3$/LaOF is the source for the gain in methane conversion and the enhancement of the C_2H_4/C_2H_6 ratio. From the O_2-TPD results obtained over the used and fresh LaOF and 10 mol% $BaCO_3$/LaOF catalysts, one can see that the surface properties of the two catalysts changed tremendously during the OCM reactions (Figs. 7 and 8). Our data suggest that new surface sites for oxygen adsorption and activation above 500°C were created during the OCM reactions. The concentration of the sites for oxygen desorption at 716°C increased with the addition of 10 mol% $BaCO_3$ and decreased when the amount of $BaCO_3$ added exceeded 20 mol%. Since the OCM reaction occurred mainly at temperatures above 700°C, we suggest that the oxygen species desorbed in the 700–750°C range were the active oxygen species for the OCM reaction. The correlation of the existence of this O_2-TPD peak (Fig. 8) and the increased in methane conversion in the 5–20 mol% $BaCO_3$ range (Fig. 1) also suggests that these oxygen species were responsible for the rise in methane conversion within the 5–20 mol% $BaCO_3$ concentration range. As the 716–760°C oxygen desorption peak disappeared with increased $BaCO_3$ loading, the conversion of methane decreased. Based on the *in situ* Raman results obtained over the 10 mol% $BaCO_3$/LaOF catalyst at 700°C under O_2 as well as under CH_4/O_2 (2.6/1) (Fig. 6b (iv) and (v)), we conclude that the surface oxygen species causing O_2 desorption in the 716–760°C range were O_2^{2-} species. In other words, the $BaCO_3$-promoted presence of O_2^{2-} species is crucial to the gain in methane conversion over the 5–20 mol% $BaCO_3$/LaOF catalysts.

To elucidate the possible role of CO_3^{2-} generation with the enhancement of OCM activity, we examined the TPD of CO_2 on catalysts of different composition. From Fig. 9, the CO_2-TPD spectra obtained over the fresh catalysts show CO_2 desorption above 850°C. According to the XRD results in Fig. 4a, the crystal phase of $BaCO_3$ could only be detected above 40 mol% $BaCO_3$ loading; the desorption of CO_2 above 850°C detected over the 10–40 mol% $BaCO_3$/LaOF catalysts after exposure to CO_2 indicated that the adsorption of CO_2 on the surface had induced the formation of "bulk" $BaCO_3$. The LaOF as well as the 10–60 mol% $BaCO_3$/LaOF catalysts gave desorption peaks at 518 and 798°C: With the increase in $BaCO_3$ loading, the 518°C peak increased in intensity while the 798°C one changed little. Apparently, the former was due to the addition of $BaCO_3$, whereas the latter not. We also performed CO_2-TPD studies on a 10 mol% BaO/LaOF catalyst and obtained CO_2-TPD spectrum similar to that over a 10 mol% $BaCO_3$/LaOF catalyst. The result further confirmed that the $BaCO_3$ added to the 10 mol% $BaCO_3$/LaOF was converted to BaO during catalyst preparation. We assign the desorption peak at 798°C to CO_2 adsorbed on strong basic sites existed largely on the surface of LaOF. For the 518°C peak, we suggest that it was due to CO_2 adsorption on BaO produced during catalyst preparation or in the case of pure LaOF, on sites with similar strength of basicity. There were CO_2-desorption peaks observed below 500°C due to CO_2-adsorption on sites with even lower basicity. The existence of various basic sites on LaOF further supports the idea of anionic vacancies or trapped electrons being present on the LaOF catalyst. In addition to these basic sites, the presence of BaO on the surface induces a new kind of basic site. Since we detected no BaO crystal phase in our XRD studies of the $BaCO_3$/LaOF catalysts, we conclude that they were well dispersed. CO_2 adsorption on BaO sites would result in the CO_2-TPD peak at 518°C. Pure $BaCO_3$ exhibits no CO_2-TPD peak at 518°C but strong CO_2 desorption above 800°C (Fig. 9f).

It is striking to observe that the used $BaCO_3$/LaOF catalysts showed very little CO_2 desorption at 518°C (Fig. 10). Only the 10 and 20 mol% $BaCO_3$/LaOF catalysts show trace of CO_2 desorption at ca. 518°C. However, a new CO_2 desorption peak was observed at 832°C for these two catalysts. For the 40 and 60 mol% $BaCO_3$/LaOF catalysts, CO_2-TPD spectra resemble that of pure $BaCO_3$. We suggest that the basic sites that induced CO_2-desorption at 832°C over the 10 and 20 mol% $BaCO_3$/LaOF were responsible for the enhancement in methane conversion. From Fig. 4, we see no crystal phase of barium compound below 40 mol% $BaCO_3$ loading before the OCM reaction. However, after the OCM reactions, $BaCO_3$ crystal phase was detected at 30 and 40 mol% $BaCO_3$ loadings. Hence the well-dispersed BaO compounds on the 30 and 40 mol% $BaCO_3$/LaOF catalysts had sintered during the OCM reaction, generating islands of $BaCO_3$ which are bulk-like. The $BaCO_3$ decomposition temperature of these islands was above 850°C (Fig. 10). For the 5–20 mol% $BaCO_3$/LaOF catalysts, although we do not see the crystal phase of any barium compound (Fig. 4b), we suggest that the $BaCO_3$ generated in the $BaO + CO_2$ reaction sintered during the OCM reaction to become clusters of $BaCO_3$. These $BaCO_3$ clusters were intermediate in size between the well-dispersed $BaCO_3$ and "bulk-like" $BaCO_3$ and were responsible for the appearance of the CO_2-TPD peak at 832°C (Fig. 10). In other words, with the control of $BaCO_3$ loading on LaOF, one can generate $BaCO_3$ clusters that decompose within the temperature range of 700–850°C. The decomposition of $BaCO_3$ in the OCM reaction could regenerate BaO on the surface. Above 30 mol% $BaCO_3$ loading, the $BaCO_3$ islands became bulk-like and did not decompose in the temperatures adopted in the OCM reactions. We conclude that the $BaCO_3$ clusters were responsible for the existence of O_2^{2-} on the 5–20 mol% $BaCO_3$/LaOF catalysts. A plausible mechanism might be speculated:

$$BaCO_3 \xrightarrow{700-850^\circ C} Ba^{2+}(O^{2-}) + CO_2\uparrow$$

$$2\,Ba^{2+}(O^{2-}) + O_2 \rightarrow 2\,Ba^{2+}(O_2^{2-}).$$

As shown by our *in situ* Raman studies, O_2^- and O_2^{n-} species are unstable on LaOF above 700°C and their involvement in the OCM reaction should thus be limited. The addition of 5–20 mol% $BaCO_3$ on LaOF provides a means of stabilizing the O_2^{2-} and O_2^{n-} species in the OCM reaction conditions and hence enhancing the conversion of methane.

CONCLUSION

We have illustrated that the LaOF catalyst could be promoted by the addition of 5–20 mol% $BaCO_3$. A gain of ca. 40% in methane conversion was resulted with only slight decrease in C_2 selectivity. The net gain in C_2 yield was ca. 30%. After detailed characterization of the LaOF and $BaCO_3$/LaOF catalysts, we conclude that the added barium stayed largely on the surface. Below 20 mol% loading, barium dispersed well on the surface and existed mainly as BaO before the OCM reactions. During the OCM reactions, BaO reacted with the CO_2 produced and sintered to clusters of $BaCO_3$. We propose that these clusters of $BaCO_3$ decompose in the OCM reactions, providing BaO sites for O_2^{2-} generation. $BaCO_3$/LaOF catalysts with $BaCO_3$ loading larger than 20 mol% would produce bulk $BaCO_3$ on the surface which only decomposed at temperatures higher than those adopted in the OCM reactions.

ACKNOWLEDGMENTS

This project was kindly supported by the Hong Kong Baptist University (HKBU) and the Hong Kong Research Grants Council, UGC (HKBC 146/95P). We thank the State Key Laboratory for Physical Chemistry, Xiamen University, for performing (by Mr. R. Q. Long) the *in situ* Raman experiments. H. H. thanks the HKBU for a Ph.D. studentship.

REFERENCES

1. Burch, R., Squire, G. D., and Tsang, S. C., *Appl. Catal.* **46**, 69 (1989).
2. Burch, R., Chalker, S., and Loader, P., "New Frontiers in Catalysis" (L. Guczi, Ed.), Elsevier, 1992.
3. Ueda, W., and Thomas, J. M., *J. Chem. Soc., Chem. Commun.* 1148 (1988).
4. Ueda, W., Isozaki, T., Morikawa, Y., and Thomas, J. M., *Chem. Lett.* 2103 (1989).
5. Ueda, W., Thomas, J. M., Philips, M. J., and Ternan, M. (Eds.), "Proceedings, 9th International Congress on Catalysis, Calgary, 1988," Vol. 2, p. 960. Chem. Inst. of Canada, Ottawa, 1988.
6. Sugiyama, S., Matsumura, Y., and Moffat, J. B., *J. Catal.* **139**, 338 (1993).
7. Voyatzis, R., and Moffat, J. B., *J. Catal.* **142**, 45 (1993).
8. Khan, A. Z., and Ruckenstein, E., *Catal. Lett.* **13**, 95 (1992).
9. Lunsford, J. H., Hinson, P. G., Rosynek, M. P., Shi, C., Xu, M., and Yang, X., *J. Catal.* **147**, 301 (1994).
10. Otsuka, K., Hatano, M., and Komatsu, T., *Stud. Surf. Sci. Catal.* **36**, 383 (1988).
11. Conway, S. J., and Lunsford, J. H., *Appl. Catal.* **79**, L1 (1991).
12. Fujimoto, K., Hashimoto, S., Asami, K., Omata, K., and Tominaga, H., *Appl. Catal.* **50**, 223 (1989).
13. Zhou, S., Zhou, X. P., Wan, H. L., and Tsai, K. R., *Catal. Lett.* **20**, 179 (1993).
14. Zhou, X. P., Zhang, W. D., Wan, H. L., and Tsai, K. R., *Catal. Lett.* **21**, 113 (1993).
15. Au, C. T., Zhang, Y. Q., Ng, C. F., and Wan, H. L., *Catal. Lett.* **23**, 37 (1994).
16. Au, C. T., He, H., Lai, S. Y., and Ng, C. F., *J. Catal.* **163**, 339 (1996).
17. Au, C. T., Hu, Y. H., and Wan, H. L., *Catal. Lett.* **23**, 37 (1994).
18. Au, C. T., Li, X. C., Tang, J., and Roberts, M. W., *J. Catal.* **106**, 538 (1987).
19. Winter, E. R. S., *J. Chem. Soc. A* 2889 (1968).
20. Winter, E. R. S., *J. Chem. Soc. A* 1832 (1969).
21. Au, C. T., He, H., Lai, S. Y., and Ng, C. F., *J. Catal.* **159**, 280 (1996).
22. Turcotte, R. P., Sawyer, J. O., and Eyring, L., *Inorg. Chem.* **8**, 238 (1969).
23. Lin, C. H., Wang, J. X., and Lunsford, J. H., *J. Catal.* **111**, 302 (1988).
24. Iwamatsu, E., Moriyama, T., Takasaki, N., and Aika, K., *J. Catal.* **113**, 25 (1988).
25. Cotton, F. A., and Wilkinson, G., "Advanced Inorganic Chemistry," 3rd ed., pp. 206, 1057. Wiley Interscience, New York, 1972.

26. Tench, A. J., Lawson, T., and Kibblewhite, J. F. J., *J. Chem. Soc., Faraday Trans. 1* **68**, 1169 (1972).
27. Ito, T., Kato, M., Toi, K., Shirakawa, T., Ikemoto, I., and Tokuda, T., *J. Chem. Soc., Faraday Trans. 1* **81**, 2835 (1985).
28. Wang, J. X., and Lunsford, J. H., *J. Phys. Chem.* **90**, 5883 (1986).
29. Smith, P., *J. Phys. Chem.* **60**, 1471 (1956).
30. Shamir, J., Binenboym, J., and Claassen, H. H., *J. Am. Chem. Soc.* **90**, 6223 (1968).
31. Herzberg, G., "Molecular Spectra and Molecular Structure I—Spectra of Diatomic Molecules," 2nd ed. Van Nostrand, Princeton, NJ, 1950.
32. Nakamoto, K., "Infrared and Raman Spectra of Inorganic and Coordination Compounds," 3rd ed. Wiley Interscience, New York, 1978.
33. Bösch, M., and Kanzing, W., *Helv. Phys. Acta.* **48**, 743 (1975).
34. Sheppard, N., "Vibration Properties of Adsorbates" (R. F. Williss, Ed.). Springer-Verlag, Berlin, 1980.
35. Eysel, H. H., and Thym, S., *Z. Anorg. Allg. Chem.* **411**(2), 97 (1975).
36. Lever, A. B. P., Ozin, G. A., and Gray, H. B., *Inorg. Chem.* **19**, 1823 (1980).
37. Valentine, J. S., *Chem. Rev.* **73**, 237 (1973).
38. Au, C. T., and Zhou, X. P., *J. Chem. Soc., Faraday Trans. 1* **92**(10), 1793 (1996).